FAST ALGORITHMS FOR RADAR CROSS SECTION COMPUTATION OF COMPLEX OBJECTS

Juan M. Rius*, M. Vall-llossera, M. Ferrando

Dep. Teoría de la Señal y Comunicaciones
E.T.S.I.Telecomunicación
Apdo. 30002, 08080 Barcelona, Spain

Abstract

Radar cross section (RCS) of complex targets can be obtained in real time using the hardware capabilities of a high performance graphic workstation. Target geometry is modelled by a computer-aided design package. First order contribution to RCS is computed under physical optics high-frequency approximation. Real time computation is achieved through graphical processing of an image obtained with local illumination modeling of the target. Multiple scattering contribution can be obtained using radiosity algorithm, a recently developed global illumination method.

RESUME

La surface équivalente radar (SER) de cibles complexes peut être obtenue en temps réel grâce aux capacités d'une station graphique performante. La géométrie de la cible est modélisée à l'aide d'un système de CAO. La contribution de premier ordre à la SER est calculée en H.F. au moyen de l'approximation de l'optique physique. Le calcul temps réel est rendu possible par le traitememt graphique d'une image obtenue à l'aide d'un modèle d'illumination locale de la cible. La contribution de diffractions multiples est obtenue à l'aide d'un algorithme de "radiosité", une méthode récente d'illumination globale.

1 Introduction

The computation of RCS of large and complex targets usually involves different scattering mechanisms, such as specular reflection, diffraction at wedges, multiple scattering, shadowing effects, returns from discontinuities, creeping waves, etc. Classical techniques for numerical computing of RCS taking into account all these effects give very accurate results, but on the other hand, they require very long CPU run time on powerful computers.

The objective of this paper is to show that RCS computation in real time is possible with a high-performance graphic workstation. Physical optics surface integral is computed using the hardware capabilities of a graphics accelerator. Real-time computation is achieved through graphical processing of an image of the target present at the workstation screen. First-order reflections are obtained by rendering of the target with a local illumination algorithm.

Although diffraction at wedges, multiple scattering and second-order effects are not taken into account, it has been found that RCS of complex targets at high frequency is predicted with reasonable accuracy by physical optics approximation.

Multiple scattering effects can be taken into account if the image of the target on the workstation screen is rendered by a global illumination method instead of a local illumination one.

2 Target modeling

A computer aided design package for geometric modeling of solids [1] has been used for modeling target geometry. The target is described as a collection of parametric surfaces, defined with two-dimensional NURBS (non-uniform rational B-splines). Intersections between surface patches are defined by NURB trimming curves on the parametric space of the intersected surfaces.

RCS analysis packages usually describe the target in terms of facets and wedges [2]. The faceting approach has a potential limitation when a large number of facets might be required, which may exceed declared array sizes or which can lead to longer CPU run times. Parametric surface modeling of the target impose weaker storage memory requirements that the faceting approach, and the modelled surface adjusts more accurately to the real target surface.

3 First order reflections

3.1 Physical Optics

The scattered fields from an arbitrary object are described by the well-known Sttraton-Chu integral equations [3]:

$$\vec{E} = \oint_S [jK\eta(\hat{n}\times\vec{H})G + (\hat{n}\times\vec{E})\times\nabla G + (\hat{n}\cdot\vec{E})\nabla G] \; ds$$

$$\vec{H} = \oint_S \left[-jK\frac{1}{\eta}(\hat{n}\times\vec{E})G + (\hat{n}\times\vec{H})\times\nabla G + (\hat{n}\cdot\vec{H})\nabla G\right] \; ds$$

where $\hat{n}$ is the unit vector normal to the surface, K the wavenumber, η the wave impedance in the medium, and G the Green function in free space:

$$G = \frac{1}{4\pi r}e^{-jKr}$$

Physical optics is based on the tangent plane approximation [4]: if the radius of curvature of a conducting surface is greater than the wavelength, the tangential component of the magnetic field over the surface can be approximated by twice the incident one over the illuminated area, and zero over shaded regions. The integrals, therefore, extend only over the illuminated portion of the surface.

The resulting integral approximation for monostatic RCS is:

$$\sigma = \frac{4\pi}{\lambda^2}\left[\int_S \cos\theta \;\; e^{-2jKz} ds\right]^2$$

where θ is the angle between the outward surface normal and the direction of observation and z the distance to the integration surface patch ds projected on the direction of observation.

Due to its great simplicity, physical optics approximation is widely used to compute monostatic RCS, regardless it has serious defects [4]:

- It obtains only reflection from surfaces, but not diffraction at wedges.
- It fails for wide non-specular angles.
- It has no dependance on polarization.
- It yields false shadow boundary contributions, due to the artificial boundary between illuminated and shadow regions, which can be overcome by stationary phase evaluation of the integral.

3.2 Hardware Graphic Processing of RCS

The main difficulty to compute the physical optics surface integral by classical numerical techniques is the detection of shadow regions. This difficulty can be easily overcome using the hidden surface removal capabilities of a graphic workstation, which can be performed by hardware if a graphics accelerator is present. Hidden surfaces are removed comparing the distance from the observer to each pixel to be drawn with the distance of the previously drawn pixel in the same display location, stored in a portion of RAM called "z-buffer" [5].

A photorealistic drawing of the target is made from a view-point coincident with radar position, so that shadowed regions are not displayed. A directional light source is defined on the same direction as the incident wave-front. If the target surface is modelled to have only diffuse light reflection, it results that the brightness of each pixel on the drawing is equal to $\cos\theta$, where θ is the angle between the outward surface normal and the direction of observation.

Therefore, the physical optics surface integral can be evaluated as the coherent addition of the brightness of all the pixels on the display. The phase of each pixel contribution can be easily obtained from the distance to the observer stored in z-buffer.

Graphic processing has the following advantages over classical numerical techniques:

- Evaluation of surface integral independent of target complexity.
- Automatic shadowed region removal.
- CPU time independent of target complexity.
- Real-time computation if hardware graphics accelerator is used.
- Very low RAM requirements, independent of target complexity.
- Target can be modelled by parametric NURB surfaces, requiring less mass storage memory that the faceting approach, and adjusting more accurately to the real target surface.

} CPU run time

On a high performance graphic workstation with hardware graphics :elerator, the CPU run time is about 30 microseconds/pixel/angle. assical numerical techniques require much longer CPU run time: ƎCOTA package, developed by Boeing Aerospace [2], takes about 11 illiseconds/facet/angle for each polarization on a VAX 11/785, including ffraction at wedges, multiple scattering and second-order effects.

.4 Results

In order to validate the graphic processing of the surface integral, the esults obtained for simple objects are compared with analytic evaluation of physical optics integral. Fig. 1 shows RCS of an ellipsoid compared vith the theoretical geometrical optics expression $\sigma = \pi \rho_1 \rho_2$, where ρ_1 ınd ρ_2 are the principal radius of curvature at the specular reflexion point. The agreement is very good.

Fig. 2 shows normalized RCS (σ / λ^2) for a circular right cylinder. Analytic physical optics results are 23.2 dB for the circular cap (0°), and 26.5 dB for the cylindric surface (90°). According to aperture antenna theory, first RCS nulls must be located at 15.3° for the circular cap, and 90° - 3.6° for the cylindric surface. The agreement with graphical processing results is excellent.

A generic missile model has been used to validate the physical optics results for complex radar targets at high frequency. Fig. 3 shows the graphic processing results, as well as RECOTA predictions [2] and measured RCS. Although wedge diffraction and multiple reflexions are not computed by graphic processing, main RCS contributions and nulls are correctly detected.

Fig. 4 shows the performance of the physical optics approximation when diffraction at wedges is present. The target is a NACA 3317 wing. The radius of curvature of the leading edge is about λ, and the trailing one is a sharp wedge. Note that physical optics computation on the leading edge is accurate for both polarizations, but on the trailing one the computation agrees with measures only for the horizontal polarization. This is due to the fact that the tangent plane approximation of the induced current on a sharp wedge is closer to the real one for parallel polarization than for the perpendicular one.

In fig. 5 the results obtained for a Boeing 727 aircraft are compared with full-scale measurements. As concluded from fig. 4 results, note that physical optics computation provides RCS peaks present on both polarizations. The graphical processing RCS has been obtained in real time (3 seconds/angle), while classical numerical techniques require several hours due to the large size of the target (128 λ).

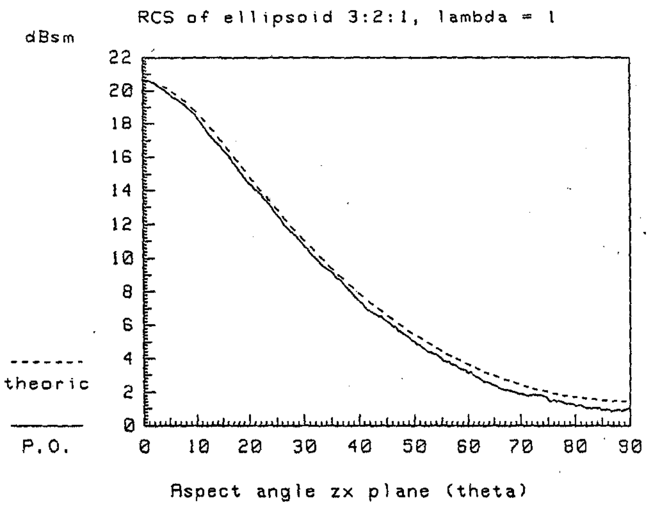

Fig. 1: Physical optics graphical processing RCS of an ellipsoid of semiaxis 3, 2 and 1 meters, $\lambda = 1$ meter, compared with geometrical optics theorical formula.

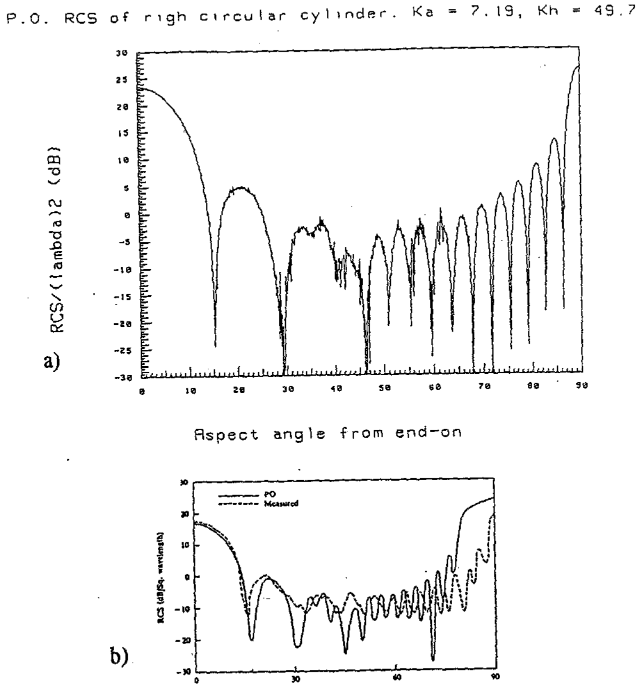

Fig. 2: RCS of a circular right cylinder of radius 1.14 λ and height 7.91 λ, at a frequency of 10 GHz.
a) Physical optics graphical processing
b) Physical optics classical numerical computation compared with experimental measurements

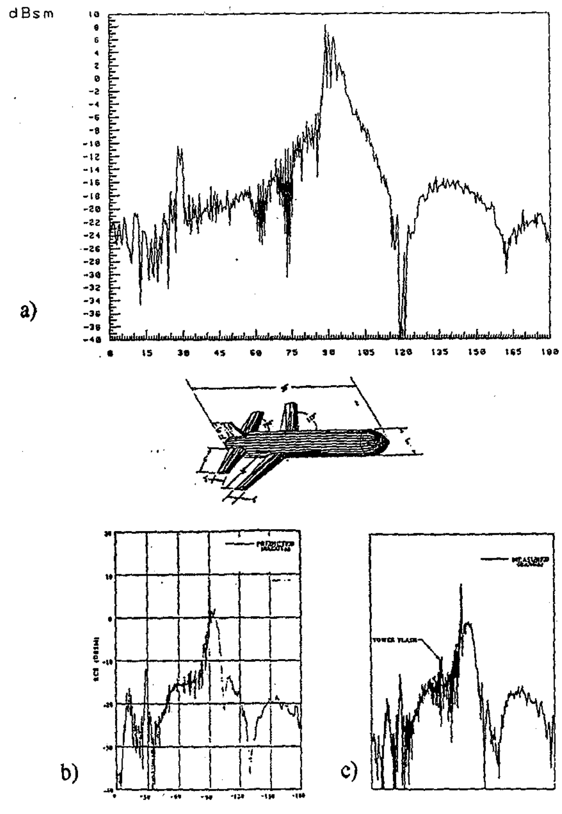

Fig. 3: RCS of missile of 1 m. length at 12 GHz
a) Physical optics graphical processing
b) RECOTA computation
c) Measured RCS for vertical polarization

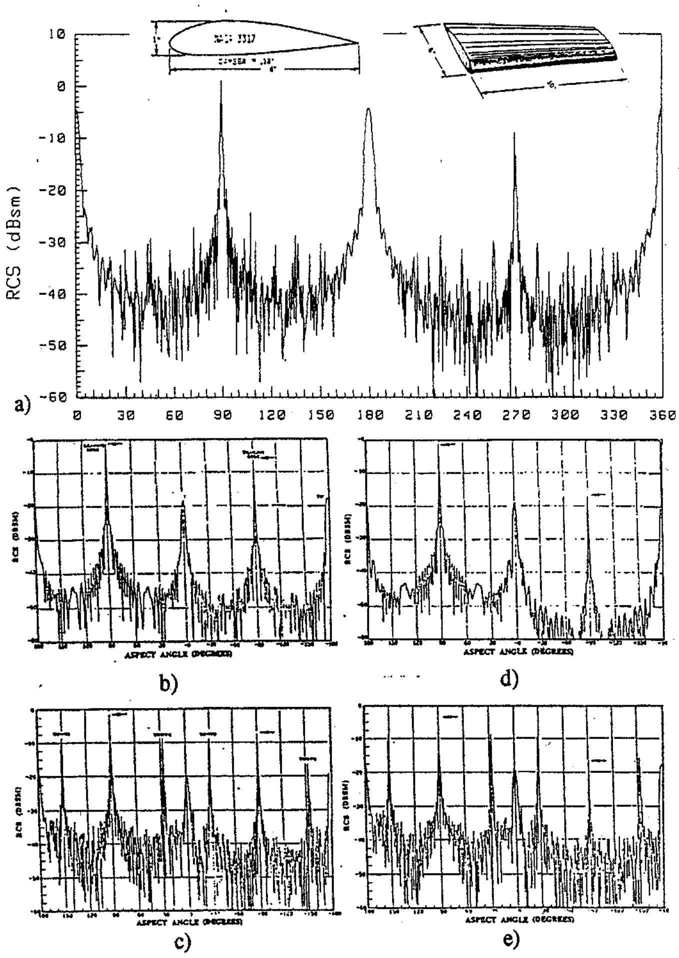

Fig. 4: RCS of NACA 3317 wing at a frequency of 16 GHz
a) Physical optics graphical processing
b) RECOTA computation for horizontal polarization
c) Measured RCS for horizontal polarization
d) RECOTA computation for vertical polarization
e) Measured RCS for vertical polarization

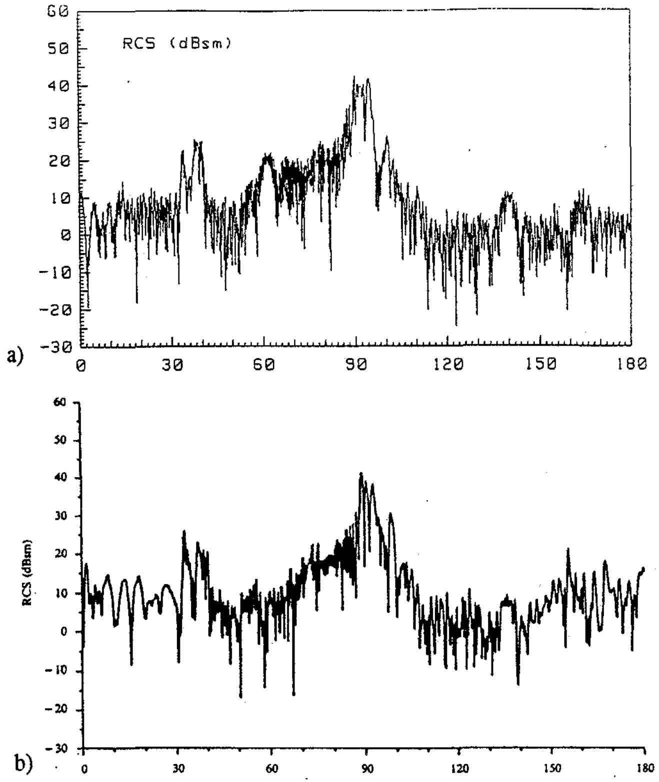

Fig. 5: RCS of Boeing 727-100C at 0.94 GHz
a) Physical optics graphical processing
b) Measured RCS for horizontal polarization

4 Multiple scattering

A local illumination model has been used to obtain first order physical optics approximation. In local illumination models only incident light from light sources and object surface orientation are considered in determining the intensity of reflected light. In global models, the light that reaches an object by reflection from other surfaces in the scene environment is also considered.

Obviously, a global illumination model must be used in order to compute multiple scattering contribution to RCS. The most popular global model is the well-known technique of ray-tracing, but unfortunately it requires a prohibitive computational cost.

Another global illumination method is the radiosity method, introduced by Goral and others [6]. This method models the interaction of light between perfectly diffuse surfaces, with a reduced computational effort.

4.1 Global Illumination Graphical Processing

The radiosity method deals with the equilibrium of radiant energy within the scene: the energy by unit time and area leaving a surface consist of direct emission from the surface plus the reflected portion of the light arriving at the surface, which is found by summing the contributions from all the other surfaces, and from the surface itself if it is concave. Considering all surfaces, we have a system of linear equations where the unknowns are the energy leaving each surface. Due to the specific nature of this system of equations, it can be solved in quasi-real time by a very fast iterative algorithm of progressive refinement [7].

Due to the incoherent nature of the radiosity method, based on an energy equilibrium basis, RCS with multiple scattering must be obtained as the incoherent addition of first order physical optics contribution plus multiple scattering radiosity contribution:

$$RCS = RCS_{P.O.} + RCS_{M.S.}$$

The last term is computed as the incoherent addition of each pixel multiple scattering contribution:

$$RCS_{M.S.} = \frac{K}{\lambda^2} \sum_{pixels} (L_r - L_0)^2$$

where L_r and L_0 are respectively the pixel intensities with radiosity method and with the local illumination model.

4.2 CPU run time

The results obtained by radiosity graphical processing require a CPU time of about 10 to 50 times slower than first order physical optics graphical processing. Although this is not a truly real time algorithm, it is still much faster than classical multiple scattering methods, so we can consider it a quasi-real time algorithm.

4.3 Results

Fig. 6 shows that multiple scattering contribution is a secondary effect when curved (not flat) surfaces are present. First order physical optics computation agree very well with RECOTA and experimental measurements.

The RCS computed by radiosity method for a dihedral is compared with experimental measurements and physical theory of diffraction in fig. 7, while fig. 8 shows the radiosity graphical processing, RECOTA computation and measured RCS of two unconnected facets. In both cases, the agreement is excellent.

Finally, fig. 9 compares the radiosity results for a complex object (missile of fig. 3) with first order physical optics and experimental measures. Note that first order RCS is lightly smaller than the measured one at angles between 50° and 70°, in which a double reflexion occurs between the fuselage and the leading edge of the wing. Note also that due to the incoherent nature of radiosity method, it can not predict phase cancellations on reflected fields, so that RCS nulls disappear.

5 Conclusions

- First order physical optics approximation predicts with reasonable accuracy RCS of real radar targets.
- Real-time results are possible with hardware graphical processing.
- Diffraction at sharp wedges can be approximated by physical optics results when the incident polarization is parallel to the wedge.
- Although multiple reflection effects are of secondary importance when RCS of real targets is computed, they can be included if a global illumination method is used for graphical processing. Due to the incoherent nature of radiosity algorithm, it can not predict phase cancellations on reflected fields, so that RCS prediction is always in excess of the measured one.

6 References

[1] *"IDEAS Geomod user's guide"*, Structural Dynamics Research Corp. (SDRC), Milford, OH 45150.

[2] *"Radar Cross Section of Complex Targets"*, Nazih N. Youssef, IEEE Proc., vol. 77, no. 5, may 1989, pp. 722-734

[3] *"Electromagnetic Theory"*, J.A. Stratton, McGraw-Hill, New York, 1941

[4] *"Radar Cross Section"*, E.F. Knot et al., Artech House, Inc. 1985

[5] *"Computer Graphics for Engineers"*, B.R. Dewey, Harper & Row Inc., 1988

[6] *"Modeling the Interaction of Light Between Diffuse Surfaces"*, C.M. Goral, K.E. Torrance, D.P. Greenberg, B. Battaile, ACM Computer Graphics, Proceedings of SIGGRAPH 1984

[7] *"Global Illumination Modeling Using Radiosity"*, D.A. Burgoon, Hewlett-Packard Journal, December 1989.

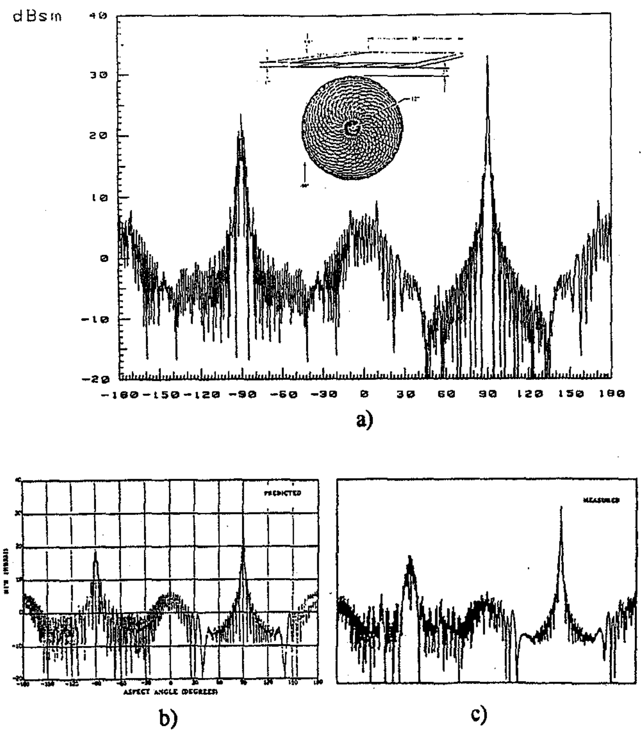

Fig. 6: RCS of a sphere (r = 10 λ) and a vertical flat plate (17 λ x 25 λ) at 10 GHz
a) Physical optics graphical processing
b) RECOTA computation
c) Measured RCS for vertical polarization

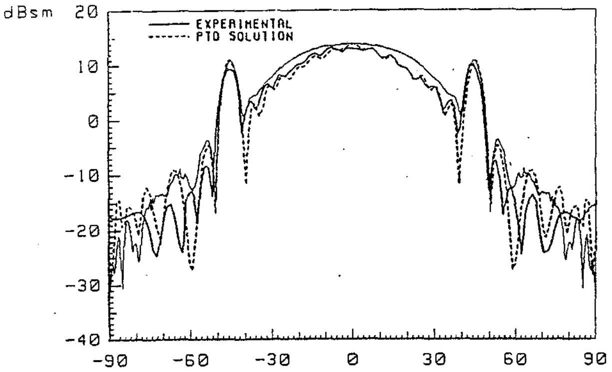

Fig. 7: RCS of 90° dihedral, (5.6 λ x 5.6 λ plates) at 9.4 GHz
Thin line: Radiosity graphical processing
Thick line: Experimental measurement
Dot line: Physical theory of diffraction

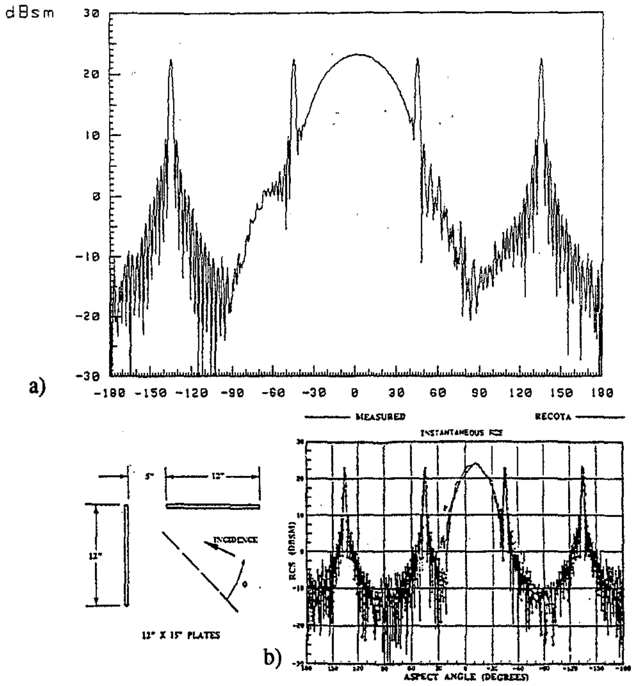

Fig. 8: RCS of unconnected facets (12" x 15" plates) at 10 GHz
a) Radiosity graphical processing
b) RECOTA computation and experimental measurement

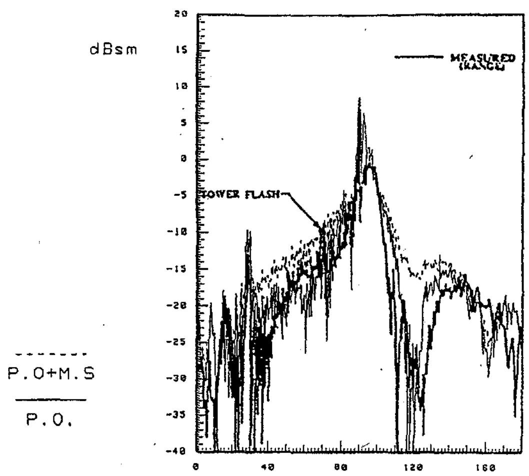

Fig. 9: RCS of missile of 1 m. length at 12 GHz
Dot line: Radiosity graphical processing
Thin line: Physical optics graphical processing
Thick line: Experimental measurement